Materials Letters 228 (2018) 96–99

Contents lists available at ScienceDirect

Materials Letters

journal homepage: www.elsevier.com/locate/mlblue

Featured Letter

LiYGeO$_4$: Novel low-permittivity microwave dielectric ceramics with intrinsic low sintering temperature

Kai Cheng [a,c], Chunchun Li [a,b,*], Huaicheng Xiang [a], Yihua Sun [c], Liang Fang [a,*]

[a] Guangxi Universities Key Laboratory of Non-ferrous Metal Oxide Electronic Functional Materials and Devices, College of Material Science and Engineering, Guilin University of Technology, Guilin 541004, China
[b] College of Information Science and Engineering, Guilin University of Technology, Guilin 541004, China
[c] College of Materials and Chemical Engineering, Three Gorges University, Yichang 443002, China

ARTICLE INFO

Article history:
Received 26 April 2018
Received in revised form 27 May 2018
Accepted 28 May 2018
Available online 1 June 2018

Keywords:
Ceramics
Dielectrics
Low permittivity
Olivine structure
Low-temperature co-fired ceramics

ABSTRACT

Using the solid-state reaction route, a new low-firing microwave dielectric ceramic LiYGeO$_4$ was prepared, and the phase evolution, thermal stability, and dielectric properties were characterized. A single orthorhombic phase LiYGeO$_4$ formed in the sintering temperature range of 920–960 °C decomposed into Y_2GeO_5, GeO_2, and Li_2O when the sintering temperature exceeded 960 °C. LiYGeO$_4$ densified at 940 °C/6 h possessed a relative permittivity 9.41, a quality factor 18,860 GHz (at 12.8 GHz), and a temperature coefficient of resonant frequency −27.7 ppm/°C. The negative τ_f value was compensated by compositing with CaTiO$_3$, and 0.97LiYGeO$_4$-0.03CaTiO$_3$ ceramic exhibited a near-zero τ_f of −1.37 ppm/°C along with a permittivity of 9.83 and a quality factor of 12,940 GHz (at 13.2 GHz). All merits make LiYGeO$_4$ a promising candidate for high-frequency communication application, and low-temperature co-fired ceramics.

1. Introduction

Recently, the explosive growth of communication technologies has expanded the operating frequency to millimeter wave range to fulfill the quantity and speed of data transmission [1,2]. Transmission speed is importantly related to the signal propagation that is positively correlated with the relative permittivity [3]. Hence, low-ε_r ($\varepsilon_r < 1\ 5$) dielectric ceramics available are strongly demanded to avoid signal propagation delay and also to minimize the cross-coupling with conductors. Moreover, low-temperature co-fired ceramics (LTCC) technology offers benefits in the fabrications of miniature multilayered devices, which also need low-ε_r materials as subtracts [4]. Hence, low-ε_r materials with high performances are strongly demanded in high-frequency and LTCC applications.

Over the past decades, some olivine structured materials A_2BO_4, e.g., Li_2AGeO_4 (A = Zn, Mg), M_2GeO_4 and M_2SiO_4 (M = Zn, Mg), have been reported as promising candidates for low-ε_r dielectric materials [5–9]. It is safe to speculate that their low permittivities derive from low ionic polarizability of the constitution ions, such as Si (0.87 Å^3) and Ge (1.63 Å^3). Besides, most of the low-ε_r materials have high sintering temperature or large $|\tau_f|$ values, which would to some extent restrict their practical applications. Furthermore, Li-containing oxides have been reported as low-firing ceramics, e.g., Li_4WO_5, $Li_4Mg_3Ti_2O_9$, and $Li_2ZnGe_3O_8$ [10–12]. Therefore, a Li-containing olivine compound LiYGeO$_4$ was prepared and characterized to seek low-ε_r dielectric materials with intrinsic low sintering temperature. The phase evolution, thermal stability, sintering behavior, and microwave dielectric properties were investigated in detail.

2. Experimental

LiYGeO$_4$ ceramics were prepared by the solid-state method and the processing procedure is similar as described in our previous work (details in supplementary information) [6]. Before weighting, Y_2O_3 powders were dried at 1000 °C for 2 h. The calcining temperature was 880 °C, and the sintering temperature ranged from 920 °C to 1000 °C for 6 h with a heating rate of 5 °C/min. Composite ceramics between LiYGeO$_4$ and CaTiO$_3$ were prepared with general formula $(1-x)$LiYGeO$_4$-xCaTiO$_3$ $(0 \le x \le 0.045)$ to adjust the thermal stability, which sintered in the temperature range of 900–960 °C for 6 h.

---

* Corresponding authors at: Guangxi Universities Key Laboratory of Non-ferrous Metal Oxide Electronic Functional Materials and Devices, College of Material Science and Engineering, Guilin University of Technology, Guilin 541004, China (C. Li).

E-mail addresses: lichunchun2003@126.com (C. Li), fanglianggl001@aliyun.com (L. Fang).

https://doi.org/10.1016/j.matlet.2018.05.124
0167-577X/

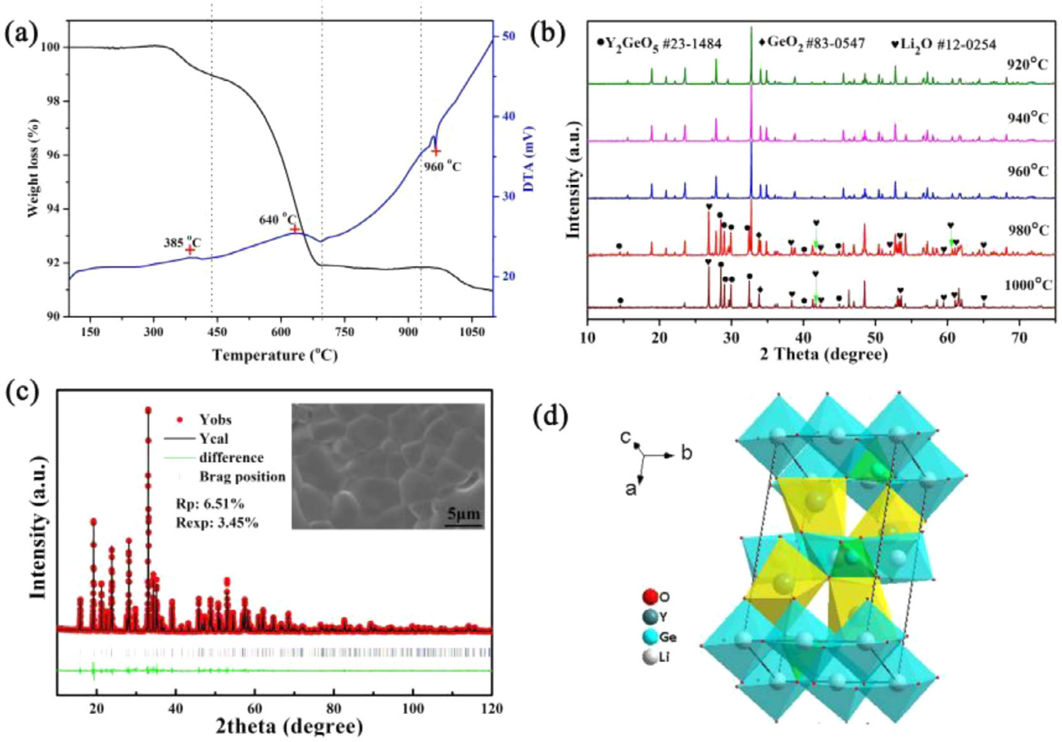

Fig. 1. (a) TGA/DSC curves of the mixture of raw powders; (b) XRD patterns of $LiYGeO_4$ ceramics; (c) Rietveld refinement and the SEM image on the sample sintered at 940 °C; (d) crystal structure of $LiYGeO_4$.

3. Results and discussion

Fig. 1a displays the TG and DTA curves on the as-milled raw powders. Three loss steps with a total weight loss of 9.3% are observed in the TG curves. An exothermic peak located at 385 °C with 1.3% weight loss was due to the decomposition of the organic species and volatilization of the adsorbed water introduced from the milling process. Similar phenomena were previously reported in the synthesis of $Mg_{0.95}Zn_{0.05}TiO_3$ and $Ba(Co_{0.7}Zn_{0.3})_{1/3}Nb_{2/3}O_3$ [13,14]. The second weight loss of 7.2% between 440 and 680 °C, accompanied by another exothermic peak at 640 °C, was ascribed to the chemical reaction of reactants. The third weight loss in the TG curve was just 0.8% but with a remarkable endothermic peak in the DTA curve at 960 °C, which probably corresponded to the thermal decomposition of $LiYGeO_4$.

XRD patterns of the as-sintered ceramics at different temperatures are shown in Fig. 1b. When sintered at 920–960 °C, $LiYGeO_4$ crystallized in a single orthorhombic phase with a space group *Pnma* (62) within the limitation of the XRD. However, additional peaks belonging to Y_2GeO_5, GeO_2, and Li_2O evidently appeared at 980 °C. These results indicate the structural instability of $LiYGeO_4$ that decomposes at the elevated temperature which is expressed as $2LiYGeO_4 \overset{Heat}{\rightarrow} Y_2GeO_5 + GeO_2 + Li_2O$. The analysis obtained from the XRD patterns coincides well with the thermal analysis.

Fig. 1c displays the Rietveld refinement (based on the CIF data No. SD031487) plots of the 940 °C-sintered sample. The low residual factors (R_{wp} = 9.03%, R_{exp} = 3.45%, and R_p = 6.51%) combined with the good match between the observed and calculated XRD patterns verified the phase purity. The refined lattice parameter and unit cell volume were refined as a = 11.3568(4) Å, b = 6.4024 (2), c = 5.1072(4), and V = 371.35(4) $Å^3$, respectively. A dense and homogeneous microstructure with clear grain boundary is observed (Fig. 1c) for the 940 °C-sintered samples, with average grain size about 7 μm. Fig. 1d shows the schematic framework of the crystal structures of $LiYGeO_4$, composed of $[GeO_4]$ tetrahedra, $[LiO_6]$ and $[YO_6]$ octahedra. The edge-sharing $[LiO_6]$ octahedra form a chain along b axis, one of which is alternating edge-linked by $[GeO_4]$ tetrahedra to another chain, resulting in layers parallel to (1 0 0) plane and $[YO_6]$ octahedra are the consecutive layers between two successive layers.

Fig. 2 illustrates the room-temperature Raman spectra of $LiYGeO_4$ ceramics, and factor group analysis indicated that the $LiYGeO_4$ crystal possessed 36 Raman-active vibrational modes as follows:

$$\Gamma_{Raman} = 11A_g + 7B_{1g} + 11B_{2g} + 7B_{3g} \qquad (2)$$

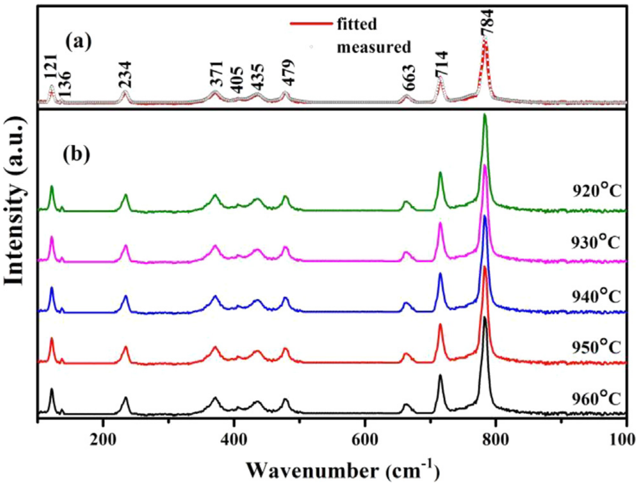

Fig. 2. Room-temperature Raman spectrum for the $LiYGeO_4$ samples in the range of 100–1000 cm^{-1} and fitting results on the sample sintered at 940 °C as a representative.